CHEMICAL ENGINEERING TRANSACTIONS

VOL. 66, 2018

A publication of AIDIC
The Italian Association of Chemical Engineering
Online at www.aidic.it/cet

Guest Editors: Songying Zhao, Yougang Sun, Ye Zhou

ISBN 978-88-95608-63-1; **ISSN** 2283-9216

DOI: 10.3303/CET1866176

Seismic Performance of High Toughness Cementitious Composite Enhanced by Carbon Fibre Reinforced Polymer Bars

Tao Cai, Shiyong Jiang*, Xueyang Li, Hongwei Gong

Department of Military facilities, Army Logistics University of PLA, Chongqing 401331, China
jiangshiy@163.com

This paper aims to disclose the seismic performance of high toughness cementitious composite (HTCC) enhanced by carbon fibre reinforced polymer (CFRP) bars. To this end, several horizontal cyclic loading tests were carried out on CFRP-enhanced HTCC columns and CFRP-enhanced ordinary concrete columns at three different axial compression ratios. Then, the test results were discussed in details with the aid of hysteresis curves and skeleton curves. The results show that the structures are much less prone to brittle failure after the ordinary concrete was replaced with the HTCC; the HTCC is much more ductile than the ordinary concrete; when the axial compression ratio was between 0.2 and 0.5, using the HTCC instead of ordinary concrete can enhance the deformation performance and energy dissipation of structures at a high axial compression ratio, thus improving the seismic performance. The research findings provide new insights into the seismic performance of the HTCC column enhanced with CFRP bars.

1. Introduction

U Corrosion of steel bars poses a serious threat to the safety and durability of structures (Fasnakis et al., 2016; Yeh et al., 2002; He et al., 2011). The threat is particularly prominent in corrosive environments (e.g. marine, jungle and wetland). What is worse, the steel is a magnetic material that may cause magneto static problems, making it dangerous to apply steel bars in buildings (e.g. observatories, telecom towers, and radar stations) that allows no electromagnetic interference. Thus, it is meaningful to find a replacement for steel bars that is corrosion-resistant and non-magnetic. One of the most viable substitutes is carbon fiber reinforced polymer (CFRP), an extremely strong and light fiber-reinforced plastic which contains carbon fibres. This material is not magnetic and strongly resistant to corrosion.

These advantages of the CFRP can be magnified by replacing the ordinary concrete with high toughness cementitious composite (HTCC) (Baena et al., 2009; Mohamed et al., 2014; Affif et al., 2014;). The HTCC is a novel composite between short monofilament fibers and cement substrate (Pereira et al., 2012). The fibers are randomly distributed in all three dimensions, such that the material exhibits significant quasi-strain hardening under tensile load (Ha et al., 2013; Li, 2001; Sharbatdar et al., 2003;). Previous studies (Lee and Li, 2014; Ouyang et al., 2013; Li and Xu, 2010) have shown that the HTCC boasts much better toughness, tensile property, bending resistance and shear performance than ordinary concrete. It is an ideal material to curb concrete deformation, crack propagation and brittle failure.

So far, there has been few reports on the seismic performance of the HTCC column enhanced with CFRP bars. To make up for the gap, this paper carries out horizontal cyclic loading tests to compare the seismic performance of CFRP-enhanced HTCC column with CFRP-enhanced ordinary concrete column.

2. Experimental design

2.1 Specimen design

As shown in Figure 1, each test column has a length of 1,175mm and a section of 250mm×250mm. With the shape of an inverted T, the column was enlarged at the top face to install a horizontal actuator. Both the

longitudinal bars and stirrups are CFRP bars.
According to the *Code for Seismic Design of Buildings* (Song and Zheng, 2012), the axial compression ratio of our tests was set to 0.2, 0.4 and 0.5, respectively. Then, the HTCC columns are denoted as H-0.2, H-0.4 and H-0.5, respectively, based on their specific axial compression ratios. Similarly, the ordinary concrete columns are denoted as C-0.2, C-0.4 and C-0.5, respectively.

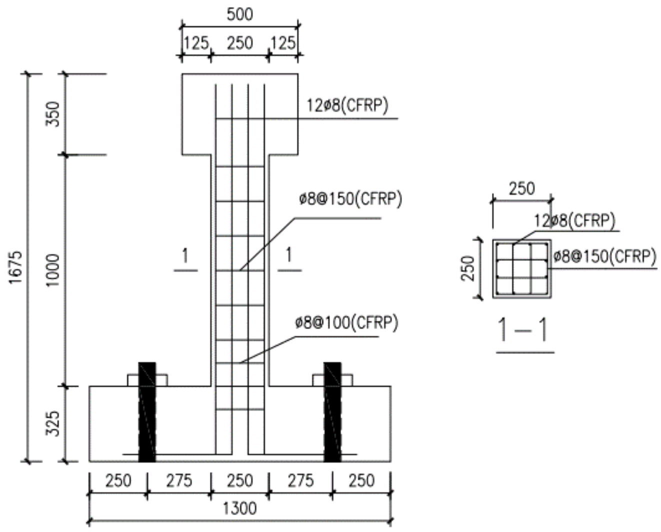

Figure 1: Specimen design

2.2 Mechanical properties

Besides pouring the test columns, the author produced several standard prism-shape compressive specimens according to the *Standard for Test Method of Mechanical Properties on Ordinary Concrete* (Tang, 2003). These specimens were subjected to compressive test to measure their axial compressive strengths. Table 1 lists the axial compressive strengths of HTCC and ordinary concrete; Table 2 presents the main mechanical parameters of CFRP bars. It can be seen that there is no big difference in axial compressive strength between the HTCC and ordinary concrete. Thus, seismic performance of the specimens has little to do with the axial compressive strengths of the materials.

Table 1: Axial compressive strength of HTCC and ordinary concrete

Specimen NO.	Measured value of compressive strength /MPa			Axial compressive strength value /MPa
H-0.2	29.9	28.1	31.5	29.8
H-0.4	31.8	29.8	32.9	31.5
H-0.5	24.3	26.2	28.6	26.4
C-0.2	30.8	29.4	31.8	30.7
C-0.4	31.0	30.9	30.5	30.8
C-0.5	26.3	31.3	31.6	31.3

Table 2: Mechanical parameters of CFRP bars

Tensile strength /MPa	Tensile modulus of elasticity /GPa	Compressive strength /MPa	Compressive modulus of elasticity /GPa
1307.6	127.2	611.1	100.2

2.3 Loading and measurement

The loading tests were carried out on a multi-channel electro-hydraulic servo pseudo-dynamic testing machine (Figure 2).
First, each test column was applied with a vertical load, which is controlled by force. After that, the horizontal actuator was connected to the column. The horizontal load is controlled by displacement. There are three stages of horizontal loading: the pre-cracking stage, the post-cracking stage, and the constant load stage. In the pre-

cracking stage, the displacement was increased by 0.5mm after each loading cycle until the first transverse crack appeared. In the post-cracking stage, the displacement was increased by 3.0mm after each three loading cycles until the horizontal load stopped to increase. In the constant load stage, the displacement was increased by 5.0mm after each three loading cycles until the horizontal load dropped to 85% of the peak load or the specimen was damaged (the termination condition).

Figure 2: Loading device

3. Test Phenomenon and Results

3.1 Test phenomenon

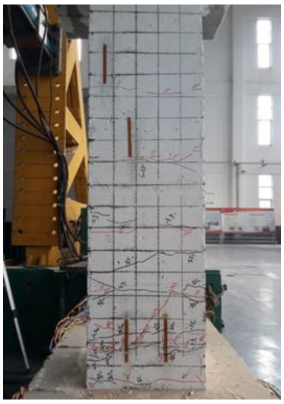

(a) H-0.2

(b) H-0.4

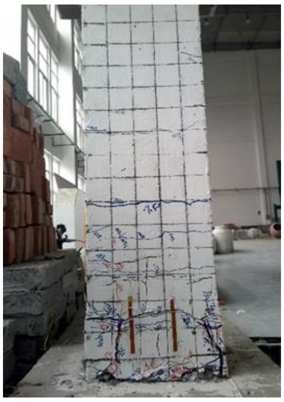

(c) H-0.5

(d) C-0.2

(e) C-0.4

(f) C-0.5

Figure 3: The destroyed mode of specimens

As shown in figure 3, the three HTCC columns shared similar trend in the failure process. The initial transverse crack appeared on the tensile side of the specimen at 8~12cm away above the bottom. Then, more and more fine transverse cracks emerged in the vicinity of the specimen. With the continued increase of horizontal displacement, the transverse cracks propagated to the sides, and the oblique cracks started to appear. At the end of the second stage, an obvious crackling sound was heard, a signal of the severe damage of the CFRP bars. Further increase of displacement was accompanied by the emergence of vertical cracks. For safety, the loading was terminated when the horizontal load dropped to 85% of the peak value. At this moment, the specimen was seriously damaged, yet none of the HTCC columns suffered from collapse or exfoliation. After the loading, severe damages were observed on the longitudinal CFRP bars.

Under the same axial compression ratio, the crack displacement of ordinary concrete column was slightly below that of the corresponding HTCC column. Besides, the cracks in ordinary concrete column were initiated locally and did not propagate as those in HTCC column. The ordinary concrete column also gave off a crips crackling sound, but the concrete in the specimen had already been crushed before that. Compared with the HTCC column, the ordinary concrete column had fewer and sparser transverse cracks, and more serious exfoliation at the root.

3.2 Hysteresis curves

Figure 4 compares the hysteresis curves of horizontal load-induced displacement between the HTCC column and the ordinary concrete column at the same axial compression ratio.

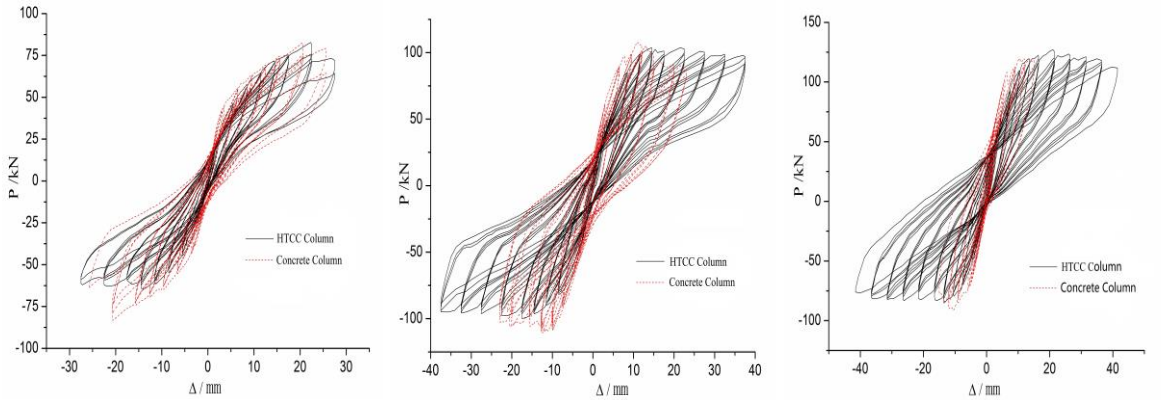

(a)n=0.2 *(b)n=0.4* *(c)n=0.5*

Figure 4: Hysteresis curves

The following trends can be derived from the figure above. There was little difference in the hysteresis curves between HTCC column and orindary concrete column in the early phase of loading.

The pinch phenonmenon was observed on all hysteresis curves. The phenonmeon is more pronounced when the specimen has a small axial compression ratio. This trend can be attributed to the crack development in the cyclic loading prcess: the cracks were expanding all the way before the reverse loading; during reverse loading, those cracks closed faster under the high axial pressure in specimens of high axial compression ratio.

Moreover, the axial compression ratio is positively correlated with the ultimate load of the specimen. For the ordinary concrete column, the greater the axial compression ratio, the smaller the limit displacement; For the HTCC column, the greater the axial compression ratio, the plumper the hysteresis curve and the greater the area under the curve.

3.3 Skeleton curves

The skeleton curve describes the relationship between the peak load and peak displacement in each loading stage. The curve can vividly represent the load-displacement relation of the specimen. Figure 4 compares the load-displacement skeleton curves between the HTCC column and the ordinary concrete column at the same axial compression ratio.

As shown in Figure 5, the skeleton curves of both types of columns can be divided into two segments: the linear growth segment and the enhancement segment. Right after loading, each skeleton curve underwent an essentially linear growth. With the increase of displacement, the specimen suffered from increasingly severe plastic deformation and obvious stiffness degradation. In this case, the growth rate of load was gradually

decreasing. The difference is that the horizontal load capacity of ordinary concrete column decreased abruptly after reaching the peak load, while the HTCC column continued to withstand cyclic loading and growing deformation. During this period, the load exhibited a long, gentle descending trend.
Furthermore, the skeleton curve of ordinary concrete column was steeper than that of HTCC column in the early phase of loading, indicating that the ordinary concrete column enjoyed greater stiffness than the HTCC column at that time. This is because the ordinary concrete column has a greater elastic modulus than the HTCC column. However, as the displacement increased, the slope of the skeleton curve of the ordinary concrete column gradually approached that of the HTCC column, and even fell below the latter. This means the ordinary concrete column suffered from greater stiffness degradation than the HTCC column. The fast decline in stiffness of the ordinary concrete column is resulted from the inner damages under serious local expansion and the early crush failure of part of the concrete.

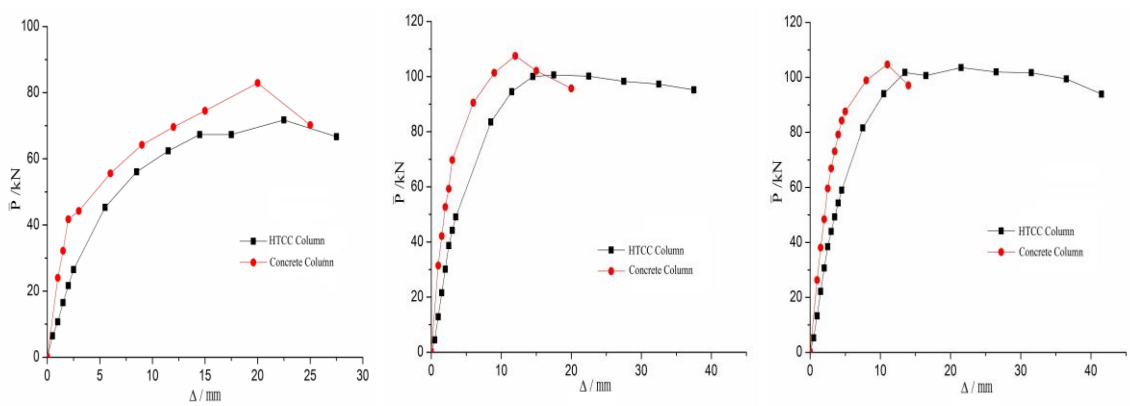

(a)n=0.2 *(b)n=0.4* *(c)n=0.5*

Figure 5: Skeleton curves

It can be found that the axial compression ratio is positively correlated with the ultimate load of the specimen. For the ordinary concrete column, the greater the axial compression ratio, the smaller the limit displacement of the specimen; For the HTCC column, the greater the axial compression ratio, the greater the limit displacement of the specimen. When the axial compression ratio was 0.2, the two types of columns had similar limit displacement. When the axial compression ratio increased to 0.4 and 0.5, the HTCC column had a much greater limit displacement than the ordinary concrete column. Therefore, the HTCC column outperforms the ordinary concrete column in deformability at a high axial compression ratio.

4. Conclusions

This paper carries out horizontal cyclic loading tests to compare the seismic performance of CFRP-enhanced HTCC column with CFRP-enhanced ordinary concrete column. The following conclusions were drawn through the comparative analysis of the test results.
Under cyclic loading, many transverse cracks appeared on both sides of the tension on the HTCC column, and the main cracks grew deeper and wider over time. However, the HTCC column did not collapse or exfoliate throughout the loading process. Despite the limited number of cracks, the ordinary concrete column experienced rapid propagation of cracks, serious exfoliation of concrete and failure of some CFRP bars. The test results prove that the structures are much less prone to brittle failure after the ordinary concrete was replaced with the HTCC.
Before the peak load, the skeleton curves of the HTCC column and the ordinary concrete column both consists of two segments: the linear growth segment and the enhancement segments. Nevertheless, after the peak load, horizontal load capacity of ordinary concrete column decreased abruptly after reaching the peak load, while the HTCC column continued to withstand cyclic loading and growing deformation. During this period, the load exhibited a long, gentle descending trend. Thus, the HTCC is much more ductile than the ordinary concrete.
For the ordinary concrete column, the deformation performance is negatively correlated with the axial compression ratio. The trend is exactly the opposite for the HTCC column. This difference shows that using the HTCC instead of ordinary concrete can enhance the deformation performance and energy dissipation of structures at a high axial compression ratio, thus improving the seismic performance. Note that this conclusion only applies to the range of axial compression ratio (n=0.2~0.5) in this research.

Reference

Affif M.Z., Mohamed H.M., Benmokra A.B., 2014, Strength and axial behavior of circular concrete columns reinforced with cfrp bars and spirals, Journal of Composites for Construction, 18(2), 68-70, DOI: 10.1061/(ASCE)CC.1943-5614.0000430

Baena M., Torres L., Turon A., Barris C., 2009, Experimental study of bond behaviour between concrete and frp bars using a pull-out test, Composites Part B Engineering, 40(8), 784-797, DOI: 10.1016/j.compositesb.2009.07.003

Fasnakis D., Papanikolaou S., Tsouknidas A., Maropoulos S., 2016, Premature fracture during fatigue testing of reinforced-concrete steel bars, Academic Journal of Manufacturing Engineering, 14(4), 40-44.

Ha G.J., Cho C.G., Kang H.W., Feo L., 2013, Seismic improvement of rc beam–column joints using hexagonal cfrp bars combined with cfrp sheets, Composite Structures, 95(1), 464-470, DOI: 10.1016/j.compstruct.2012.08.022

He M.J., Yang C., Cai J., Huang Y.S., Wu Y., 2011, Probabilistic evaluation of effects of column moment magnification factor on seismic performance of reinforced concrete frames, Advanced Materials Research, 243-249, 251-257. DOI: 10.4028/www.scientific.net/AMR.243-249.251

Li Q., Xu S., 2010, Experimental research on mechanical performance of hybrid fiber reinforced cementitious composites with polyvinyl alcohol short fiber and carbon textile, Journal of Composite Materials, 45(1), 5-28, DOI: 10.1177/0021998310371529

Li V.C., 2001, Tensile strain-hardening behavior of polyvinyl alcohol engineered cementitious composite, Aci Materials Journal, 98, 483-492.

Mohamed H.M., Afifi M.Z., Benmokrane B., 2014, Performance evaluation of concrete columns reinforced longitudinally with frp bars and confined with frp hoops and spirals under axial load, Journal of Bridge Engineering, 19, DOI: 10.1061/(ASCE)BE.1943-5592.0000590

Ouyang W., Geng G.L., Lin M., Yu X.Q., 2013, Experimental research on mechanical properties of cement based composites pva fiber reinforced, Applied Mechanics & Materials, 454, 242-245, DOI: 10.4028/www.scientific.net/AMM.454.242

Pereira E.B., Fischer G., Barros J.A.O., 2012, Direct assessment of tensile stress-crack opening behavior of strain hardening cementitious composites (SHCC), Cement & Concrete Research, 42(6), 834-846, DOI: 10.1016/j.cemconres.2012.03.006

Sharbatdar M.K., 2003, Concrete columns and beams reinforced with frp bars and grids under monotonic and reversed cyclic loading, Dissertations & Theses.

Song C., Zheng H.J., 2012, Introduction to asce7 seismic design and the comparison with Chinese code GB 50011-2010, Applied Mechanics & Materials, 238, 881-885.

Tang X.M., 2003, What i learn from the execution of testing methods for the mechanical performance of common cement′ GB/t 50081-2002, Physical Testing & Chemical Analysis Part A Physical Testing.

Tosun-Felekoğlu K., Felekoğlu B., Ranade R., Lee B.Y., Victor C.L., 2014, The role of flaw size and fiber distribution on tensile ductility of pva-ecc, Composites Part B Engineering, 56(1), 536-545, DOI: 10.1016/j.compositesb.2013.08.089

Yeh Y.K., Mo Y.L., Yang C.Y., 2002, Seismic performance of rectangular hollow bridge columns, Journal of Structural Engineering, 128(1), 60-68, DOI: 10.1061/(ASCE)0733-9445(2002)128:1(60)